

Spectral hole-burning study of magnetic and hyperfine interactions in $\text{SrF}_2:\text{Pr}^{3+}:\text{D}^-$ and $\text{CaF}_2:\text{Pr}^{3+}:\text{D}^-$

R. J. Reeves* and R. M. Macfarlane

IBM Research Division, Almaden Research Center, 650 Harry Road, San Jose, California 95120-6099

(Received 11 June 1992)

In $\text{SrF}_2:\text{Pr}^{3+}$ and $\text{CaF}_2:\text{Pr}^{3+}$ single crystals into which hydrogenic ions such as D^- have been diffused, persistent spectral hole burning occurs due to motion of neighbor hydrogenic ions following resonant excitation of Pr^{3+} . We have used both this hole burning and optically detected magnetic resonance, as high-resolution probes of the magnetic and hyperfine structure of the ground state of several sites containing different configurations of hydrogenic ions. For these sites the pseudoquadrupole splittings range from 25–633 MHz and the nuclear-moment enhancement factors from 9–350 times that of the bare nuclear moment of Pr^{3+} . The observations are well described by a Hamiltonian including Zeeman and hyperfine interactions within the lowest two electronic levels.

I. INTRODUCTION

The system consisting of trivalent praseodymium ions doped in CaF_2 and SrF_2 crystals into which H^- , D^- , or T^- ions have been diffused, exhibits a form of spectral hole burning caused by H^- (or D^- , T^-) motion in the lattice following resonant excitation of the f - f transition of the Pr^{3+} ion.^{1–5} The relaxation of the excited Pr^{3+} ions is dominated by nonradiative processes involving local mode vibrations of nearby hydrogenic ions. The resulting motion of these ions gives rise to persistent spectral holes in the Pr^{3+} absorption line, which have lifetimes of at least several hours at low temperatures. In addition, hole burning also occurs by the more usual process of optical pumping of the praseodymium hyperfine levels.

Excitation with a broadband laser ($\Delta\nu \approx 1 \text{ cm}^{-1}$) excites the entire spectral line and results in the formation of a stable photoproduct center whose absorption frequency can be shifted by as much as 50 cm^{-1} from the original site.⁵ Such excitation leads to a bleaching of the total fluorescence with characteristic time scales of the decay, ranging from a few seconds to several minutes, depending upon the particular center under study. Additionally, for some of the centers, the loss of absorption can be recovered by a simple switching of the laser polarization to the orthogonal orientation.^{1,5}

The predominant hydrogenic center in these crystals is the tetragonal (C_{4v}) center in which Pr^{3+} ions are charge compensated by H^- ions in vacant, body center positions along (100) directions (the " $C_{4v}\text{H}^-$ " sites). The centers of interest to us here have rhombic symmetry and are modified from the C_{4v} center by the addition of extra hydrogenic ions in the near-neighbor coordination cube. Figure 1 shows a schematic diagram of these centers containing two or three D^- ions. Persistent spectral hole burning occurs for these rhombic sites but does not occur in single hydrogenic ion C_{4v} centers.

The rhombic centers have singlet ground states because of the removal of the twofold degeneracy of the

tetragonal E level that is present in the parent C_{4v} site.⁶ Of particular interest is the fact that the various members of the family of sites differ greatly in the strength of the rhombic distortion and hence the splitting Δ of the ground state E level.⁷ This has dramatic and important consequences for the magnetic properties of the ground

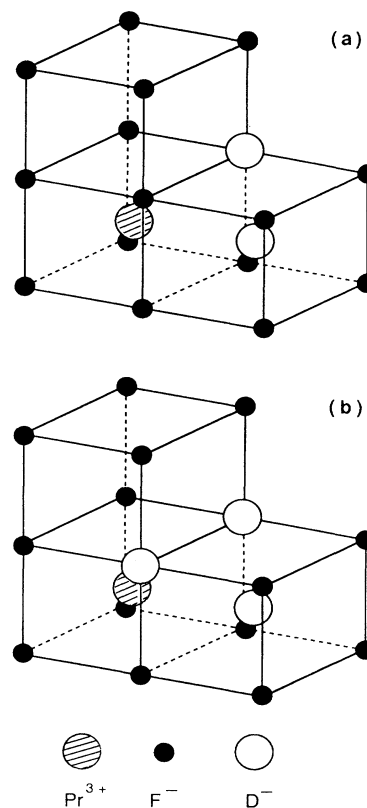


FIG. 1. Schematic representation of two classes of $\text{Pr}^{3+}:\text{D}^-$ centers in the CaF_2 structure containing (a) two and (b) three hydrogenic ions.

state of ^{141}Pr , which we investigate here. The magnetic behavior of singlet ground states is determined largely by the nuclear spin, the hyperfine coupling constant, and the off-diagonal magnetic-dipole coupling between the ground state and higher-lying electronic states. This gives rise to second-order hyperfine, or pseudoquadrupole splittings⁸ and substantial enhancements of the nuclear magnetic moment⁹ from the close-lying levels. In the study of the magnetic and hyperfine interactions presented here, we find these enhancements in the nuclear magnetic moment to be as large as a factor of 350.

II. EXPERIMENT

Crystals of CaF_2 and SrF_2 doped with 0.05% Pr^{3+} were co-doped with D^- by diffusion in a deuterium atmosphere at 850°C as described previously.⁵ It is estimated that approximately 10% of the total F^- ions in the crystals are exchanged by D^- ions. Single crystals were cut and polished with (100) faces and immersed in liquid helium at 1.6 K. Optical transitions between the ground state and the lowest crystal-field component of the $^1\text{D}_2$ multiplet were observed in absorption, fluorescence, and fluorescence excitation, using cw dye lasers with jitter-limited bandwidths of 1–2 MHz.

Spectral holes were burnt using two different schemes. For persistent holes, exposures of ≈ 3 s at ≈ 100 mW/cm^2 were made. The holes were detected by scanning the same laser about the burning frequency by ± 100 MHz to ± 10 GHz, depending on the site, and detecting the changes in sample fluorescence. For short-lived holes, one laser was used to burn a hole by optical pumping, while a second laser, with its beam coincident with the first in the sample, probed the holes, again in fluorescence excitation. An external magnetic field was applied by a split pair of superconducting coils. The field was applied parallel to the [100] axis of the crystal, and in all cases, the laser polarization E_L was perpendicular to the magnetic field.

For sites which did not exhibit persistent hole burning, transient holes were observed due to optical pumping of the hyperfine levels. These levels are separated by ~ 10 – 100 MHz and the laser radiation produces a redistribution of population as holes are burnt. The application of resonant rf radiation fills in the holes and the resulting change in fluorescence intensity is used to optical-

ly detect the nuclear resonance. In these experiments the crystal was placed inside an rf coil and the whole apparatus placed inside a liquid-helium immersion cryostat. Hyperfine splittings were determined by sweeping the rf frequency while monitoring the sample fluorescence.

III. RESULTS

Eight rhombic symmetry centers were studied in total: four in each of the crystals $\text{CaF}_2:\text{Pr}^{3+}:\text{D}^-$ and $\text{SrF}_2:\text{Pr}^{3+}:\text{D}^-$. The four centers in each crystal are designated $C_s(1)$ through $C_s(4)$,⁵ and each center is identified by its corresponding properties in the two crystals. Figure 1(a) shows the proposed model for $C_s(1)$ and Fig. 1(b) for $C_s(2)$. The properties leading to these assignments and models for the other centers are discussed in Ref. 5. The excitation wavelengths and the splittings Δ between the two lowest levels of the centers studied are listed in Table I. The effect of the rhombic distortion on the hyperfine splittings enters through the splittings Δ of the parent $C_{4v}E$ ground state.

A. Hole burning

The hole-burning spectrum for each of the centers studied is shown in Fig. 2 for $\text{CaF}_2:\text{Pr}^{3+}:\text{D}^-$ and Fig. 3 for $\text{SrF}_2:\text{Pr}^{3+}:\text{D}^-$ crystals. In each case there is a central hole at the laser frequency and, depending upon the particular site, there are six additional side holes or antiholes. The origin of the side structure is the redistribution of population among the sublevels of the ground state. These levels are split by the second-order hyperfine interaction dominated by contributions from the first excited electronic state at energy Δ above the ground state.

At 1.6 K, the hole-burning character was persistent for the $C_s(2)$ center in both crystals and for the $C_s(1)$ center in $\text{SrF}_2:\text{Pr}^{3+}:\text{D}^-$. For these cases, the optical excitation induces a phototransformation of the center that shifts the Pr^{3+} ion absorption to another wavelength or polarization, and the side structure is a hole pattern as all levels of the ground state are depleted (Figs. 2 and 3). The remaining centers exhibit transient holes at 1.6 K and, as shown in Figs. 2 and 3 for the $C_s(3)$ and $C_s(4)$ centers, the side structure is observed as antiholes. Here the mechanism is optical pumping of the hyperfine levels,

TABLE I. Spectral and magnetic hyperfine data for the C_s centers in $\text{CaF}_2:\text{Pr}^{3+}:\text{D}^-$ and $\text{SrF}_2:\text{Pr}^{3+}$.

Crystal	Center	Wavelength (nm)	Δ (cm^{-1})	g (MHz/G)	$2D_{\text{obs}}$ (MHz)	$2D_{\text{calc}}$ (MHz)	Enhanced moment (kHz/G)
CaF_2	$C_s(1)$	601.24	0.53	2.48	633	865	920
	$C_s(2)$	604.79	9.5	2.46	52	51	52
	$C_s(3)$	606.40	18.5	2.75	32	32	32
	$C_s(4)$	602.29	20.2	2.61	26.9	26.7	28
SrF_2	$C_s(1)$	598.40	3.3	2.50	164	150	155
	$C_s(2)$	601.80	8.3	2.45	64	57	59
	$C_s(3)$	603.46	16.3	2.69	32	35	36
	$C_s(4)$	599.82	21.3	2.56	24.9	24.4	25

and antiholes are observed corresponding to enhanced absorption from levels that receive population. At temperatures above 5 K, all centers under study exhibit persistent hole burning. It was under such conditions that the spectrum of the $C_s(1)$ center in $\text{CaF}_2:\text{Pr}^{3+}:\text{D}^-$ [Fig. 2(a)] was recorded and side holes are observed.

Figure 4 shows a schematic energy-level diagram for the rhombic symmetry centers. The nuclear spin of ^{141}Pr is $I=5/2$, giving three hyperfine levels in zero magnetic field, split in the ratio of 2:1 in axial symmetry. The approximation of axial symmetry is well satisfied here as the centers retain a large measure of the tetragonal symmetry of their parent center. With singlet electronic states, the first-order hyperfine interaction is quenched, and the Hamiltonian consists of the pseudoquadrupole term

$$H = D^g e [I_z^2 - I(I+I)/3] + E^g e [I_x^2 - I_y^2], \quad (1)$$

where g, e refer to ground and excited states. We consid-

er only interactions between the two lowest electronic states (Z_1 and Z_2) and since these states largely retain their tetragonal E character, only the z component of the magnetic-dipole operator is important and the smaller of the two hyperfine splittings is given by

$$2D = \frac{2A_f^2 |\langle \phi^+ | J_z | \phi^- \rangle|^2}{\Delta}, \quad (2)$$

where ϕ^+ and ϕ^- label the electronic levels. The strongest transitions will conserve M_I and the predicted pattern of holes is shown in the lower part of Fig. 4. The central hole is expected to have three times the intensity of the side holes.

The expected seven-hole pattern is observed for the $C_s(1)$ and $C_s(2)$ centers in both CaF_2 and SrF_2 crystals [Figs. 2(a), 2(b), 3(a), 3(b)]. The variation in Δ between the sites changes the splittings between holes according to Eq. (2) and consistent with the axial approximation be-

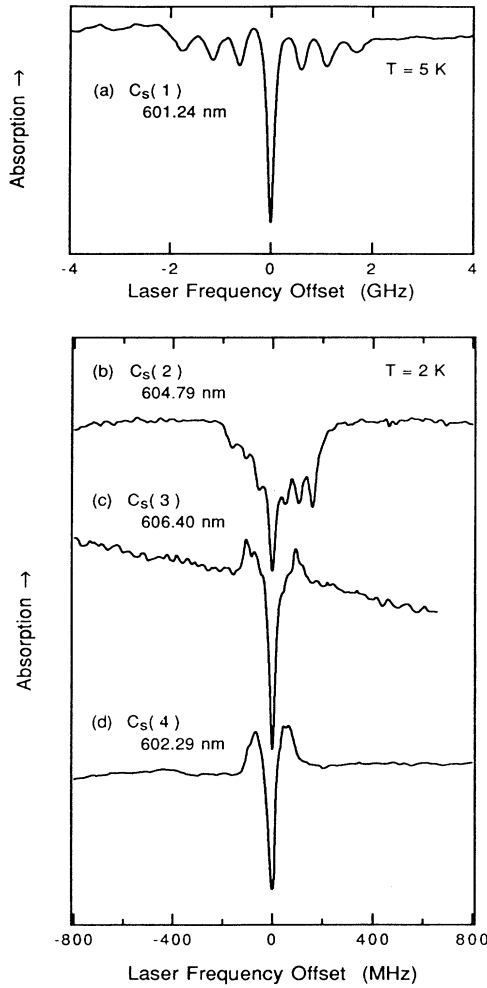


FIG. 2. Hole-burning spectra for four rhombic centers in $\text{CaF}_2:\text{Pr}^{3+}:\text{D}^-$. In (a) and (b) the holes are persistent due to D^- motion and the side structure is seen as a series of six holes. In (c) and (d) the holes arise from optical pumping of hyperfine lines and the side structure is seen as antiholes.

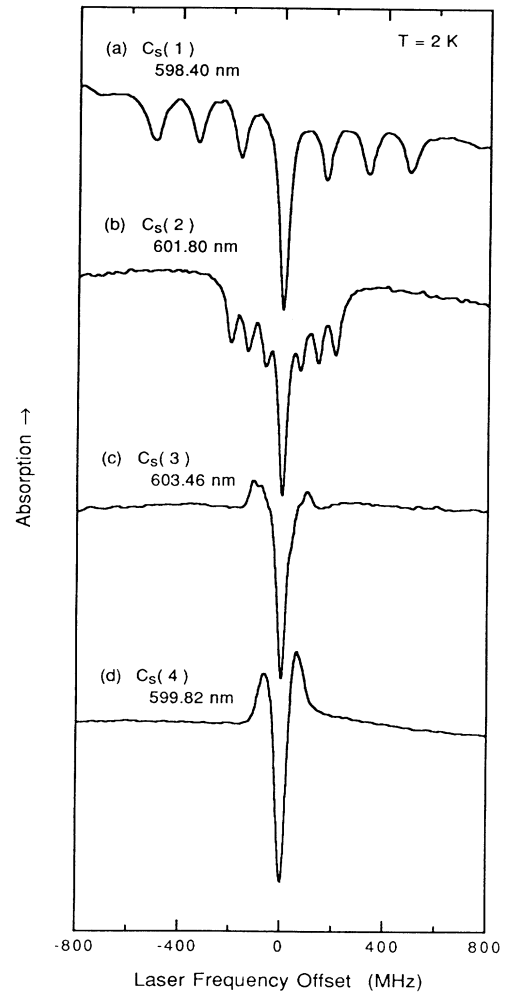


FIG. 3. Hole-burning spectra for four rhombic centers in $\text{SrF}_2:\text{Pr}^{3+}:\text{D}^-$. In (a) and (b) the holes are persistent due to D^- motion and the side structure is seen as a series of six holes. In (c) and (d) the holes arise from optical pumping of hyperfine lines and the side structure is seen as antiholes.

ing used, equal spacing within a particular center is generally observed.

B. Optically detected nuclear resonance

For the $C_s(3)$ and $C_s(4)$ centers, only transient holes could be observed at 1.6 K with hole lifetimes of a few seconds. This is characteristic of optical pumping of the hyperfine levels for which side-hole structure is present as antiholes. For the $C_s(4)$ centers, the complex antihole structure is not well resolved so the pseudoquadrupole splittings were measured using ODNMR techniques. The spectra obtained for this center in each crystal are shown in Fig. 5. The three lines observed for each site correspond to all possible transitions between the three hyperfine levels. The frequencies of the lines are 24.9, 48.0, and 73.4 MHz for $\text{SrF}_2:\text{Pr}^{3+}:\text{D}^-$ and 26.9, 53.0, and 80.0 MHz for $\text{CaF}_2:\text{Pr}^{3+}:\text{D}^-$. As expected, the sum of the first two frequencies, corresponding to transitions labeled nominally $(\pm 1/2 \rightarrow \pm 3/2)$ and $(\pm 3/2 \rightarrow \pm 5/2)$, is equal to the third frequency (nominally $\pm 1/2 \rightarrow \pm 5/2$). The degree of axial symmetry is represented by the ratio of the first two frequencies. For SrF_2 and CaF_2 , the ratios are 1.93 and 1.97, respectively, close to the value of 2.0 expected for pure axial symmetry. The measured hyperfine interaction parameters are given in Table I for all of the centers studied.

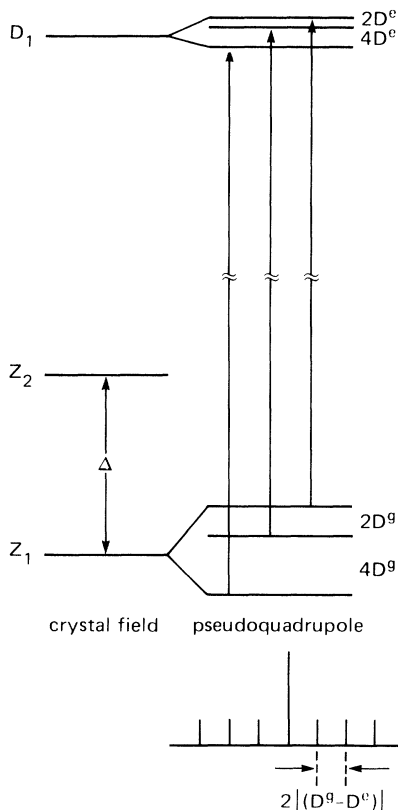


FIG. 4. Schematic energy-level diagram for the rhombic centers showing the dominant optical transitions. When these transitions remove the centers from resonance with the laser, side holes appear in the spectrum as shown.

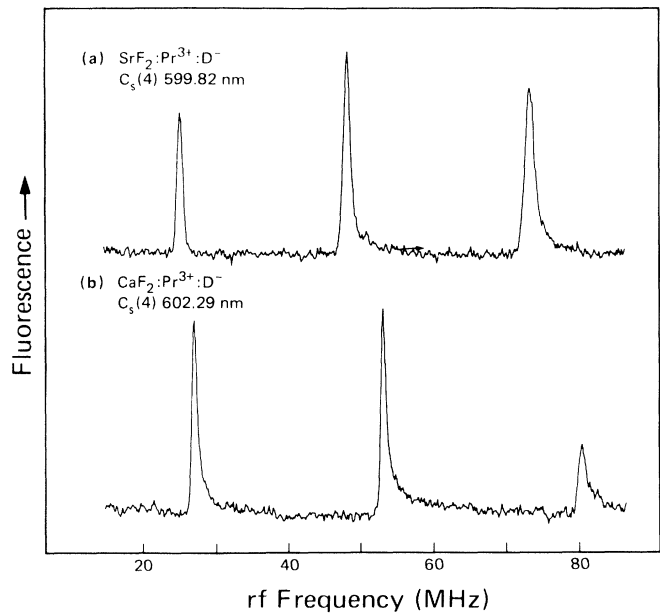


FIG. 5. Optically detected nuclear resonance for the $C_s(4)$ center at 1.6 K: (a) SrF_2 and (b) CaF_2 .

C. Nonlinear Zeeman interaction

The nonlinear Zeeman effect was studied by measuring the shift of the zero-phonon line in an external magnetic field. The line shift was monitored by fluorescence excitation and the laser was mode hopped in steps of 10 GHz

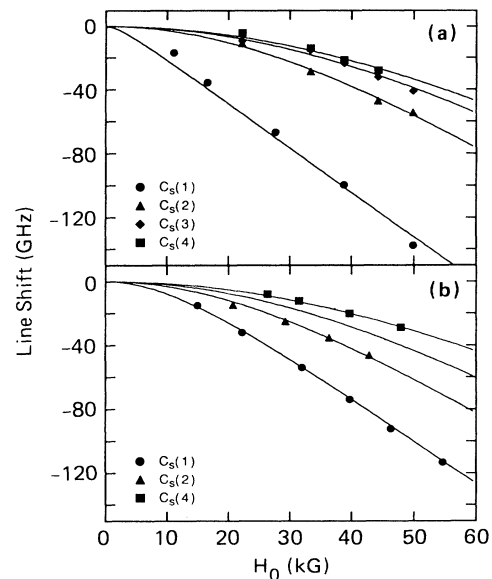


FIG. 6. Nonlinear Zeeman shift of the zero-phonon lines of four rhombic centers in (a) $\text{CaF}_2:\text{Pr}^{3+}:\text{D}^-$ and (b) $\text{SrF}_2:\text{Pr}^{3+}:\text{D}^-$. The solid curves were calculated from Eq. (7) with the off-diagonal g value as a free parameter.

as the field was increased. Seven of the eight centers under study were measured and the results are shown in Fig. 6. Note how the line shift becomes linear when it is of the same order of magnitude as Δ .

The magnetic Hamiltonian describing the system is

$$\mathcal{H} = g_J \beta \mathbf{J} \cdot \mathbf{H} + A_J \mathbf{I} \cdot \mathbf{J} + g_n \beta \mathbf{I} \cdot \mathbf{H}, \quad (3)$$

where $A_J = 1093$ MHz,¹⁰ $\beta = 1.404$ MHz/G, and $g_J = 0.8$ for the $^3\text{H}_4$ multiplet of Pr^{3+} . If ϕ^+ and ϕ^- are the two components of the ground-state E level split by energy Δ in the rhombic crystal field, the magnetic interaction between these components defines g through the equation

$$\langle \phi^+ | \mathbf{J} \cdot \mathbf{H} | \phi^- \rangle = gg_J \beta H_z \quad (4)$$

and also

$$\langle \phi^+ | \mathbf{I} \cdot \mathbf{J} | \phi^- \rangle = g A_J I_z. \quad (5)$$

$$E = \frac{\Delta}{2} - \frac{1}{2} \sqrt{\Delta^2 + (2g A_J I_z)^2 + 4g^2 g_J \beta A_J I_z H_z + (2gg_J \beta H_z)^2} \quad (8)$$

using g as an adjustable parameter for each center. The splitting of the electronic states Δ was fixed at its measured value. The values of g obtained are given in Table I and the corresponding theoretical fits are shown in Fig. 6. The sensitivity of the fitting procedure determines the g values to better than ± 0.05 . The line shift was not measured for the $C_s(3)$ center in $\text{SrF}_2:\text{Pr}^{3+}:\text{D}^-$ but a value of g was determined by comparing the ratios of g between $C_s(1)$, $C_s(2)$, and $C_s(4)$ sites in $\text{CaF}_2:\text{Pr}^{3+}:\text{D}^-$.

The results show that this model of the magnetic Hamiltonian with a single parameter g gives an excellent fit to the measured nonlinear Zeeman shifts. The g values obtained are physically reasonable, being a little less than the value of $g = 3.875$ measured for the $C_{4v}\text{F}^-$ site in $\text{CaF}_2:\text{Pr}^{3+}$.¹¹ We note that for these rhombic sites, the g value represents an off-diagonal magnetic coupling between the levels split by the rhombic perturbation. This produces a nonlinear shift rather than the normal linear splitting, but because the two lowest levels are isolated, the concept of a g value is still useful.

Using the values of g determined in the above manner, together with measured values of Δ , we obtained values for the pseudoquadrupole splittings $2D$ from the expression

$$2D = 2g^2 A_J^2 / \Delta. \quad (9)$$

The values obtained are given in Table I. There is also excellent agreement between the measured and calculated values of $2D$.

D. The Pr^{3+} -enhanced nuclear magnetic moment

Hole-burning experiments were also performed in the presence of the magnetic field and the splitting between holes was measured as a function of field. The transient hole burning of the $C_s(3)$ and $C_s(4)$ centers became per-

Neglecting the effect of the magnetic field on the nuclear spin levels, the hyperfine level energies will be given by the eigenvalues of the matrix

$$\begin{bmatrix} 0 & a \\ a & \Delta \end{bmatrix}, \quad (6)$$

where the off-diagonal term is

$$a = gg_J \beta H_z + g A_J I_z. \quad (7)$$

The eigenvalue equation will give the energies of the six hyperfine levels of each of the electronic states ϕ^+ and ϕ^- as a function of magnetic field and can be used to obtain the g value. The measured line shifts were fit to the equation for the $I_z = +1/2$ level

sistent in a field and the side structure was revealed as holes rather than antiholes. The application of the magnetic field separates the degenerate nuclear spin levels to produce the six hyperfine levels designated by the six values of the nuclear spin projection $M_I = 5/2, \dots, +5/2$. At a sufficiently high field, the spacing between levels will be more or less equal and an eleven-hole pattern will result with hole intensities expected to be in a 1,2,3,4,5,6,5,4,3,2,1 intensity ratio. Figure 7 shows the pattern obtained for the $C_s(2)$ center in $\text{CaF}_2:\text{Pr}^{3+}:\text{D}^-$ as

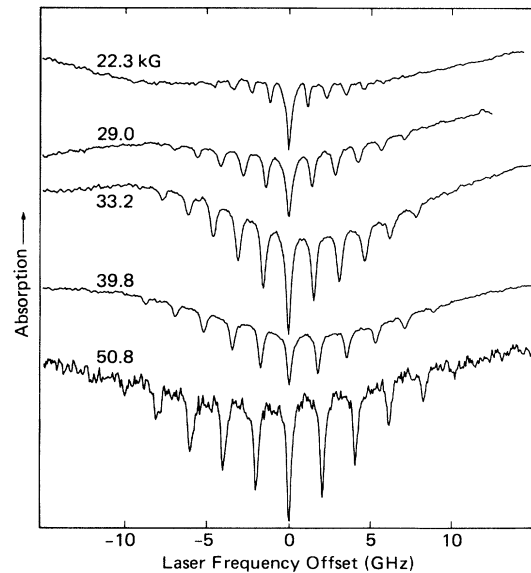


FIG. 7. Zeeman splitting of the hole spectrum of the $C_s(2)$ center in $\text{CaF}_2:\text{Pr}^{3+}:\text{D}^-$ at 1.6 K.

a function of magnetic field. Above a field of 29 kG, the expected hole pattern is observed. The results for all the centers studied are shown in Fig. 8. The $C_s(4)$ center in $\text{SrF}_2:\text{Pr}^{3+}:\text{D}^-$ was not measured.

The theoretical model used to fit the g values of the centers can also be used to model the Zeeman splitting between holes by taking the difference between adjacent I_z levels, e.g., $I_z = \pm 1/2$. The splittings were calculated in this manner for all the centers as a function of field H_0 and are shown as solid lines in Fig. 8. Considering that these splittings are calculated without any free parameters, agreement with the data is excellent. As expected, the deviation is greatest at low fields where there is considerable crossing of levels in the transition region from the seven-hole zero-field pattern to the high-field eleven-hole pattern. Figure 9 shows all six hyperfine levels of the ground electronic state for the $C_s(2)$ center in $\text{CaF}_2:\text{Pr}^{3+}:\text{D}^-$ in the low-field region. The figure shows that equal spacing between levels is not observed below fields of about 20 kG.

The behavior of the splitting for the $C_s(1)$ center in $\text{CaF}_2:\text{Pr}^{3+}:\text{D}^-$ is very different from that exhibited by the others. There is a rapid increase in hole splitting at low fields, leading to a saturation value of 2.8 GHz at high fields. When the interaction with the external field is much greater than Δ , the splitting approaches that given by the first-order hyperfine interaction [see Eq. (6)]. The small value of Δ enables this saturation value to be realized for the fields available here. The value obtained

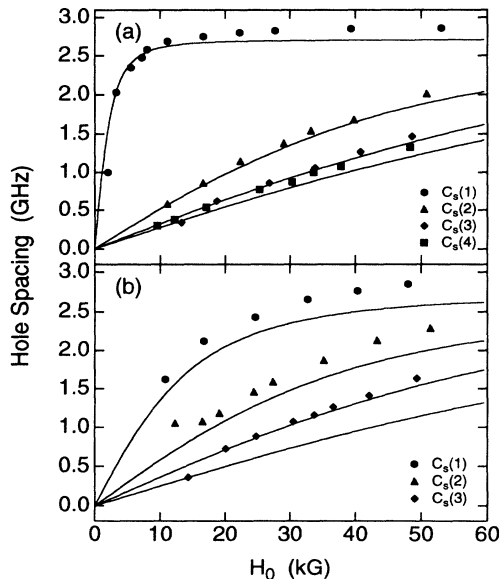


FIG. 8. Splitting between adjacent holes in the Zeeman spectrum of the four rhombic centers in (a) $\text{CaF}_2:\text{Pr}^{3+}:\text{D}^-$ and (b) $\text{SrF}_2:\text{Pr}^{3+}:\text{D}^-$. Experimentally, equal hole spacings are observed only at sufficiently high fields, with this condition depending on the particular site. The solid curves, which depict the splitting of the $\pm 1/2$ states, were calculated using g values determined from the nonlinear Zeeman effect of the zero-phonon lines.

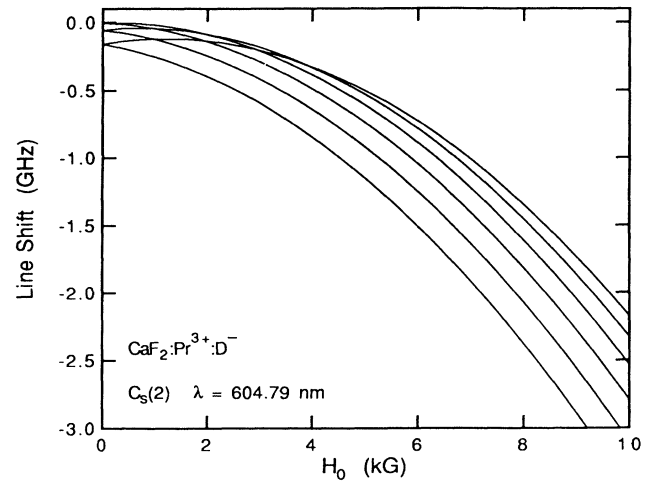


FIG. 9. Calculated Zeeman pattern for the hyperfine components of the ground state of the $C_s(2)$ center in $\text{CaF}_2:\text{Pr}^{3+}:\text{D}^-$.

is in good agreement with that of 2.85 GHz for the axial $C_{4v}\text{D}^-$ center.¹² The model is remarkable in accurately predicting this behavior.

For $\text{SrF}_2:\text{Pr}^{3+}:\text{D}^-$, the model is somewhat less satisfactory at fitting the data and consistently underestimates the splitting between holes for both the $C_s(1)$ and $C_s(2)$

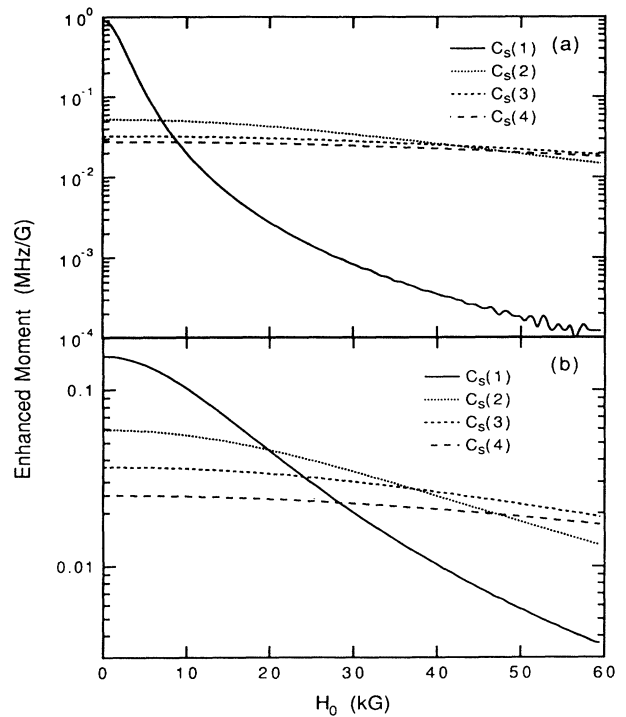


FIG. 10. Magnetic field dependence of the enhanced nuclear magnetic moment for the four rhombic centers in (a) $\text{CaF}_2:\text{Pr}^{3+}:\text{D}^-$ and (b) $\text{SrF}_2:\text{Pr}^{3+}:\text{D}^-$. These curves were obtained by differentiating the curves of Fig. 8.

centers. The $C_2(3)$ center shows a better fit, but in this case the sole parameter g was determined from a comparison with CaF_2 rather than directly from the data.

Given that the model satisfactorily explains the results obtained for the nonlinear Zeeman effect and the measured hole splittings, it can be used to give the enhanced magnetic moment that arises from the nearby electronic state. The enhanced magnetic moment can be determined from the change in the hole splitting as a function of magnetic field, i.e., it will be the derivative of the curves shown as solid lines in Fig. 8. These curves were differentiated and the results are shown in Fig. 10. The enhanced moment peaks at zero field when the two lowest electronic levels are closest together, and asymptotically approaches the value of the bare nuclear moment of Pr^{3+} at high fields. The field at which the moment approaches this value corresponds to the field at which the hole splitting appears to saturate, which occurs here only for the $C_s(1)$ center in $\text{CaF}_2:\text{Pr}^{3+}:\text{D}^-$. Because of the small value of Δ for this center, the enhanced mo-

ment is extremely large (0.7β), approaching the value of an electron moment. The values for all the centers are given in Table I.

CONCLUSION

We have studied the hyperfine interaction and magnetic properties of a family of Pr^{3+} centers in $\text{CaF}_2:\text{Pr}^{3+}:\text{D}^-$ and $\text{SrF}_2:\text{Pr}^{3+}:\text{D}^-$ in which some of the near-neighbor fluorine ions are replaced by D^- ions. The centers exhibit a form of persistent spectral hole burning in which laser irradiation in the zero-phonon line of the metastable $^1\text{D}_2$ level induces a physical motion of the D^- ion. Using this spectral hole burning, together with optically detected magnetic resonance and the nonlinear Zeeman effect, we have obtained a detailed description of the magnetic properties of these centers. We find that the magnetic properties are well described by a simple Hamiltonian with Zeeman and hyperfine interactions within the lowest pair of levels.

*Present address: Physics Department and Center for Laser Research, Oklahoma State University, Stillwater, OK 74078.

¹N. J. Cockroft, T. P. J. Han, R. J. Reeves, G. D. Jones, and R. W. G. Syme, *Opt. Lett.* **12**, 36 (1987).

²R. M. Macfarlane, R. J. Reeves, and G. D. Jones, *Opt. Lett.* **12**, 660 (1987).

³R. J. Reeves, G. D. Jones, N. J. Cockroft, T. P. J. Han, and R. W. G. Syme, *J. Lumin.* **38**, 198 (1987).

⁴R. J. Reeves and R. M. Macfarlane, *Phys. Rev. B* **39**, 5771 (1989).

⁵R. J. Reeves, G. D. Jones, and R. W. G. Syme, *Phys. Rev. B* **40**, 6475 (1989).

⁶D. P. Burum, R. M. Shelby, and R. M. Macfarlane, *Phys. Rev.*

B **25**, 3009 (1982).

⁷R. J. Reeves and R. M. Macfarlane, *J. Opt. Soc. Am. B* **9**, 763 (1992).

⁸J. M. Baker and B. Bleaney, *Proc. R. Soc. London Ser. A.* **245**, 156 (1958).

⁹B. Bleaney, *Physica* **69**, 317 (1973).

¹⁰A. Abragam and B. Bleaney, *Electron Paramagnetic Resonance of Transition Ions* (Clarendon, Oxford, 1970), p. 298.

¹¹R. M. Macfarlane, D. P. Burum, and R. M. Shelby, *Phys. Rev. B* **29**, 2390 (1984).

¹²N. B. Manson, Z. Hasan, P. T. H. Fisk, R. J. Reeves, G. D. Jones, and R. M. Macfarlane, *J. Phys. Condens. Matter* **4**, 5591 (1992).